JOURNAL OF APPLIED ELECTROCHEMISTRY 15 (1985) 745–754

Adsorption on packed bed electrodes

P. J. MAYNE*, R. SHACKLETON

The Department of Chemistry, The University, Southampton SO9 5NH, UK

Received 19 June 1984; revised 15 October 1984

The potential-dependent sorption which occurs on a graphite surface is quite different from that on metals and permits a wide range of materials from molecules to bacteria to be sorbed. The active sites for this process are the edges of the graphite layer planes where the pK of the surface functional groups is modified by the applied potential to control the sorption in a manner analogous to that on an ion exchange resin.

1. Introduction

From the earliest studies of solid–solution interfaces [1] it has been recognized that ions and molecules exhibit potential-dependent adsorption at electrodes and there is now a copious literature on the adsorption of organic compounds on metal electrodes, the most favoured for study being platinum [2] and mercury. To remove a useful weight of material from solution electrodes of very large surface area are required. This may be achieved using porous or packed bed electrodes, the theory of whose operation as electrochemical reactors is well developed [3]. The object of this work is to examine the possibility of applying potential dependent adsorption to filtration. To this end the adsorption on a packed bed electrode of a range of materials of increasing dimensions has been examined, starting with amino acids and dyes, proceeding to a protein and finally examining a bacterium; this last being frequently used as a test for the efficiency of a filter.

Previous work in this department on the electrosorption of organic contaminants from aqueous solution [4, 5] used granular activated carbon throughout [5] as the bed material and pyridine as the 'contaminant'. With no applied potential pyridine was adsorbed on the bed and little effect was observed on the adsorption by the application of a wide range of potentials. However, extreme positive and negative potentials were found to aid desorption of pyridine from the bed, the spectrophotometric analysis being complicated by the generation of hypochlorite and the breakup of the activated carbon. It was concluded that diffusion within the pores of the carbon granules was a process which increased the weight of material which might be adsorbed, but left it outside the influence of a potential change. To avoid the problems of bed breakup and diffusion within pores more dense graphite was used in this work. Morganite EY110 was chosen as being a highly developed electrographite of high density (1.8) and conductivity.

Strohl and Dunlap [6] have reported the electrosorption and separation of quinones on a column of graphite particles from a 1:1 v/v mixture of acetonitrile and water. Alkire and Eisinger [7] applied a model based on uniform surface coverage to potential dependent adsorption of β-naphthol on glassy carbon. While this type of carbon was not tested in the present work, the experimental results indicate that coverage is far from uniform on graphite.

2. Experimental details

2.1. *Electrochemical cells*

The first electrochemical cell consisted of a tube of porous Vycor glass, 1.6 cm in diameter, containing ground graphite with an axial graphite rod as feeder electrode and a platinum wire coil counter electrode round the exterior of the

* *Present address*: 16 Gower Road, Royston, Herts SG8 5DU, UK.

0021–891X/85 $03.00 + .12

Vycor tube. A salt bridge led from a point halfway down the tube and midway between the Vycor and feeder electrode to a saturated calomel reference electrode. Morganite EY110 graphite was ground in a pestle and mortar and sieved. The 250–500 μm fraction was heated to 150° C in concentrated sulphuric acid and then washed repeatedly with deionized water to remove the acid. Strohl and Sexton have reported that acid treatment improved the adsorption capacity of their graphite beds [8]. Two cells of this pattern were constructed, one with a Vycor tube 22 cm long and the other 7 cm long. Unless otherwise stated both the cell and counter electrode compartment contained nitrogen purged 0.01M Na_2SO_4. The chief differences between these and the cell of Strohl and Dunlap are the dimensions and the use of a saturated calomel reference electrode effectively positioned within the bed, not the counter electrode compartment.

Following successful tests with these Vycor tube separated cells a flat cell was constructed in which the solution and current flows were parallel. The graphite granules were contained in a graphite tube (4 cm in diameter) one end of which was closed except for seventeen 1 mm holes. Solution flowed upwards through a sintered glass disc, through the 1 mm holes in the end of the graphite tube and then through the 1 cm depth of graphite particles. Above this was positioned a further sintered glass disc and a spiral of platinum wire as the counter electrode. A salt bridge from the middle of the 1 cm deep, 4 cm diameter bed led to the reference electrode. The solution therefore flowed over both the bed and the counter electrode, unlike the Vycor tube cells. This design of cell was easier to empty and refill when different graphites, particles sizes and pre-treatments were examined.

2.2. *Detectors and potential control*

The potential of all the beds was controlled using a Chemical Electronics potentiostat type TR40-3A (Chemical Electronics Co., Newcastle upon Tyne, UK) and the concentration of the cell output was monitored continuously using an SP 700 spectrophotometer (Unicam Instruments, Cambridge, UK) or, in the case of the colloidal and particulate dispersions, a nephelometer.

The nephelometer was constructed from a 1 cm^2 square section flow-through cell with two side compartments containing glycerine to reduce the refractive index change in the incident light path and thus diminish the background scattered light in the cell. A 36 W car headlamp bulb positioned 30 cm from the cell was focused on it through one of the glycerine compartments, and the light scattered at right angles focused onto an EMI 9781 B side window photomultiplier also positioned 30 cm from the cell. The signal from the photomultiplier was recorded on a Mosley Autograph model 680M recorder. When using the nephelometer all solutions had to be filtered through a 0.45 μm millipore filter to reduce the background scattered light. A reservoir of supporting electrolyte was held approximately 0.6 m above the bench, and the solution was permitted to flow by gravity through the Vycor tube cell, then to the spectrophotometer or nephelometer, via a needle valve through a rotameter and finally to waste.

2.3. *Tests with bacteria*

A subculture of *Serratia marcescens* from the National Collection of Type Cultures no. 1377 was grown on slopes of Oxoid Lab-lemco agar. Slopes of 48 hours were washed into the supporting electrolyte reservoir with filtered water through an 8 μm millipore filter to ensure removal of large aggregates of agar, bacteria etc.

To test the viability of the bacteria the cell depicted in Fig. 1 was used in conjunction with a flow meter and a reservoir of nitrogen-purged solution. The cell consisted of two beds (5 cm diameter, 1 cm deep) of 250–500 μm graphite granules separated by a sintered glass disc, i.e. two of the flat bed cells described above, one acting as the counter electrode to the other. No reference electrode was incorporated and it was found that with 0.01 M Na_2SO_4 solution in the cell up to 4 V could be applied between the beds before gas evolution occurred.

The apparatus was initially sterilized with a solution of 0.01% sodium metabisulphite in 0.05 M sulphuric acid and then washed with 500 ml of sterile 0.01 M Na_2SO_4 solution to

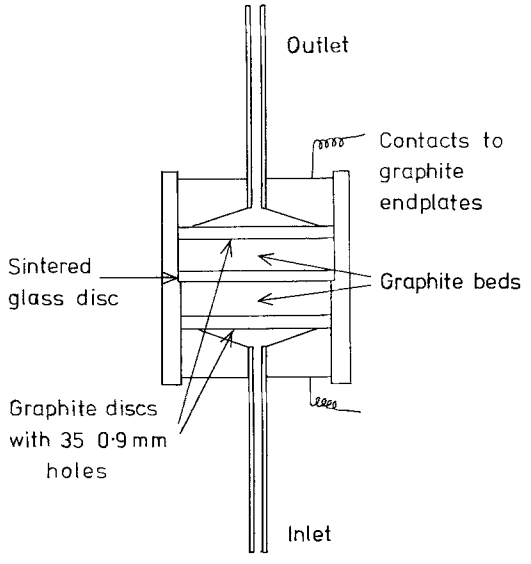

Fig. 1. Twin bed cell. Two beds 1 cm deep and 5 cm diameter of 250–500 μm graphite granules were separated by a sintered glass disc.

remove traces of acid and SO_2. A sample of the effluent was then collected and cultured on Lablemco agar to ensure that the sterilization process had been effective, the results of the whole run being discarded if any bacteria were detected at this stage.

To the reservoir of sterile, nitrogen-purged 0.01 M Na_2SO_4 was added 1% of a slope of *Serratia marcescens*, and 200 ml of solution was allowed to flow via the cell to waste to ensure that the cell was uniformly infected. No potential was applied to the cell at this stage. Nine sterile 10 ml flasks collected the next 90 ml of solution from the cell. Following the filling of the first flask 4 V was applied across the cell and the polarity was reversed every minute until the sixth flask was full when the potential source was disconnected and the final three flasks filled with no potential applied. Nine sterile pipettes were used to transfer 1 ml from each flask to sterile agar solution which was poured into sterile petri dishes, incubated for 2 days and the resulting colonies counted.

3. Results

3.1. *OH^- ion, amino acid and dye sorption*

Since pure solutions may be used one might expect no inherent difficulty with the use of the spectrophotometer in the UV to follow the concentration of any material with a simple unconjugated chromaphore. However, when using the spectrophotometer at 202 nm a desorption peak was always obtained at -1.0 V, the height of which increased with the preceding period for which the bed was held at $+0.2$ V. Moreover, this desorption at -1.0 V was not eliminated by the use of filtered water or by the further reduction of the solution oxygen concentration with a Hersch scrubber [9]. (The reservoir of supporting electrolyte was normally purged with white spot nitrogen blown through a sintered disc in the solution.)

Runs with solutions of different pH suggested that OH^- ions were the species adsorbed and desorbed and to confirm this a glass electrode was positioned in the solution flow downstream from the spectrophotometer. Fig. 2A shows the percentage transmission at 202 nm with time. A potential change was made at the packed bed every 5 min from $+0.2$ V to -1.0 V and vice versa. The double spike in the centre of the trace was produced by a potential step -1.0 V to 0.0 V followed by a second step 0.0 V to $+0.2$ V. The solution was 10^{-2} M Na_2SO_4 + 10^{-3} M NaOH flowing at 16.9 ml min^{-1} through the short Vycor tube cell. Fig. 2B shows the response of the pH electrode: it can be seen that all the increases in transmission are accompanied by a decrease in pH and vice versa. The close matching of the two traces proves that OH^- ions are adsorbed and desorbed on the packed bed. The potential changes are too small for the discharge of OH^- ions to cause the pH change; besides, were this the case a plateau would be observed, not peaks in the pH and percentage transmission curves. The instrumental readings when the supporting electrolyte was run directly to them bypassing the Vycor tube cell were 100% transmission and pH 10.8. So it appears that there is a background continuous adsorption of OH^- ions, or possibly leaching of H^+ ions from the bed of graphite.

The blank signal from OH^- ion adsorption and desorption therefore precluded measurement in the UV below about 250 nm. A variety of molecules in different supporting electrolytes was tried to avoid this difficulty. Fig. 3 shows

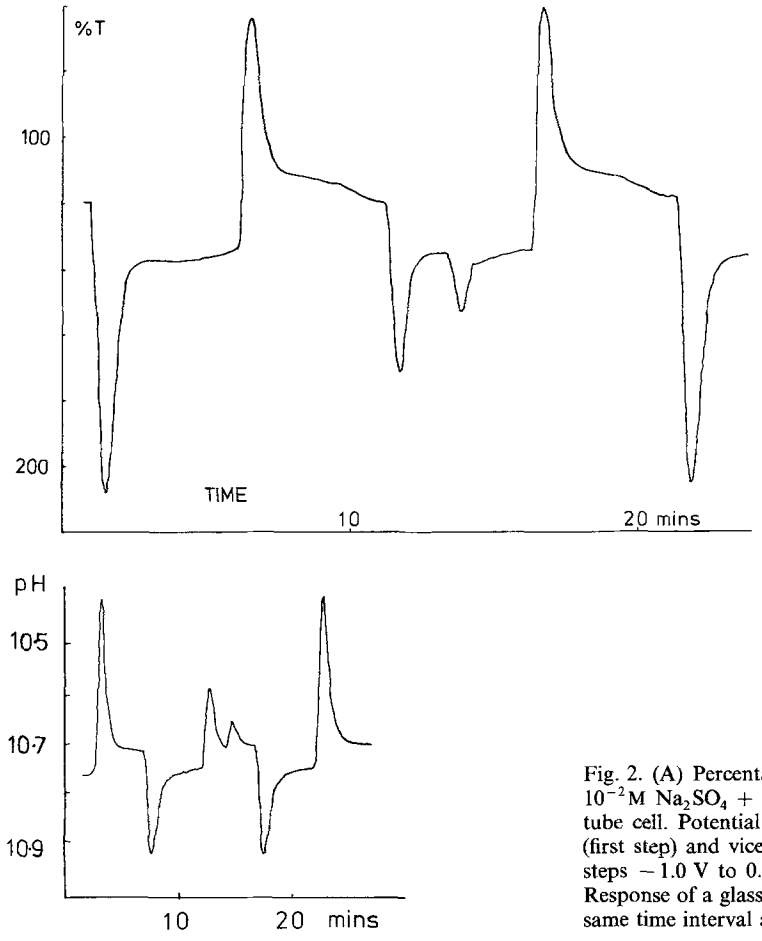

Fig. 2. (A) Percentage transmission at 202 nm vs time of 10^{-2}M Na_2SO_4 + 10^{-3}M NaOH leaving the short Vycor tube cell. Potential steps every 5 min −1.0 V to +0.2 V (first step) and vice versa. Double spike produced by two steps −1.0 V to 0.0 V followed by 0.0 V to +0.2 V. (B) Response of a glass electrode to the same solution over the same time interval as Fig. 2A.

the desorption of rhodamine B into 1M H_2SO_4, following adsorption from that solvent. In this case desorption was most marked at +1.0 V. The figure shows clearly the growth of the desorption peak with increasing periods of adsorption at −0.33 V so that considerable concentration of the feedstock solution could be achieved.

The amino acids tyrosine and tryptophan have unsaturated rings with UV absorption maxima at 274 and 278 nm respectively; they were also adsorbable and desorbable from the graphite bed. The potentials of adsorption and desorption were strongly pH-dependent (see Table 1) but the phenomenon still occurred at the isoelectric pH of the amino acid indicating

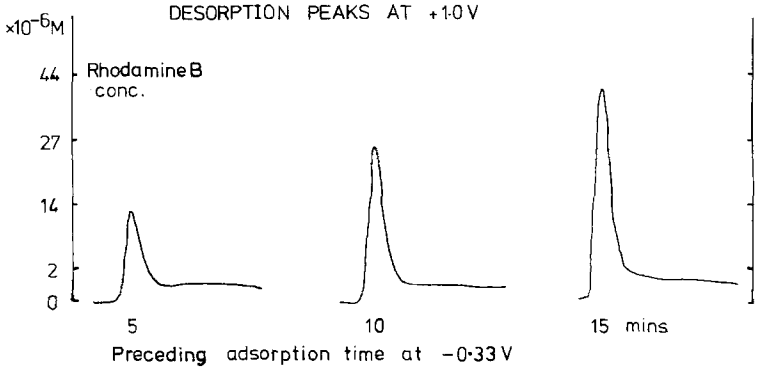

Fig. 3. Desorption of rhodamine B into 1 M H_2SO_4 following 5, 10, and 15 min adsorption at −0.33 V.

Table 1. Potentials of adsorption and desorption of amino acids

	Potential of adsorption (V)	*Potential of desorption (V)*
Tyrosine in 0.1 M H_2SO_4	−0.1	+0.8
Tyrosine in pH 5.6 acetate buffer	+0.8	−1.0
Tryptophan in 0.1 M H_2SO_4	−0.2	+1.2
Tryptophan in pH 5.9 acetate buffer	+0.5	−0.9

that electrophoresis plays no part in the mechanism of retention.

3.2. *Protein sorption*

The protein lysozyme contains eight tryptophan residues and consequently has a band in its absorption spectrum at 282 nm. Fig. 4 shows its adsorption and desorption on the graphite bed from 0.01 M Na_2SO_4. It can be seen that the bed is slowly being saturated during the adsorption phase so that the rate of adsorption decreases and the height of the subsequent desorption peak is not directly proportional to the adsorption time. The potentials of adsorption and desorption were not as specific as was found for the amino acids. In general a negative potential step encouraged adsorption, while a positive one encouraged desorption. Consequently at 0.0 V desorption occurred if a step was made from −1.0 V, while adsorption occurred when the step was from +1.0 V.

A bed-loading weight was determined from curves such as those of Fig. 4 by converting the percent transmission to absorbance point by point and using Simpson's rule to obtain the areas under the curve up to the point where the depletion or discharge of lysozyme was half its maximum. Combining this area with the volumetric flow rate gave the weight of adsorbed protein.

These loading figures were used to determine the retention of protein on the bed. The weight of lysozyme desorbed following adsorption over 5 min was measured, and the experiment was repeated interposing elution over 10 min with protein-free supporting electrolyte between the adsorption and desorption. During the period of elution the potential was maintained at the adsorption potential. From these two weights a retention percentage was calculated. The results of these measurements made at two adsorption–desorption potentials and three lysozyme concentrations with the short Vycor tube cell are given in Table 2. The retention is always close to 100% and the loading is independent of potential. A potential-dependent feature not evident in the table is the rate of desorption which was markedly faster at +0.8 V than +0.4 V, producing sharper desorption peaks, i.e. greater concentration of the effluent. The loading measurements were repeated with the longer Vycor tube cell and more concentrated protein solutions with the results given in Table 3.

The dry weight of graphite in the larger cell was 30.5 g compared with 9.5 g in the smaller cell, i.e. 3.2 times as much, whereas the average loading on the larger cell was 3.7 times the smaller. No definite trend emerges of increasing loading with concentration even over a concentration change of an order of magnitude. The results indicate that the loading of protein is

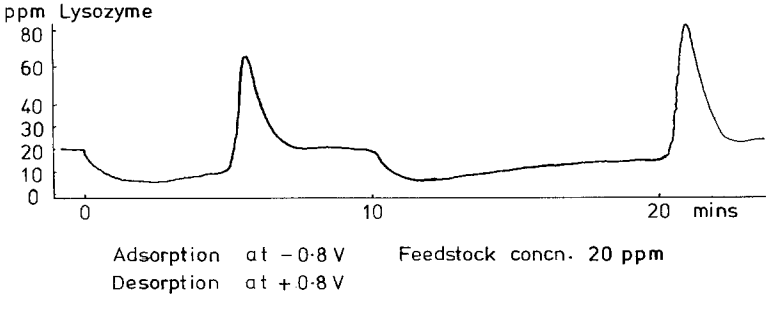

Fig. 4. Adsorption and desorption of lysozyme from a 20 ppm solution in 0.01 M Na_2SO_4.

Table 2. Weights of lysozyme adsorbed and retained in the small cell

Method	*Solution concentration (ppm)*	*Flow rate (ml min^{-1})*	*Loading (mg)*	*Retention (%)*
Adsorbing at −0.8 V, desorbing at +0.8 V	10	11.1	1.0	127
	20	10.9	0.9	93
	40	10.6	1.1	99
Adsorbing at −0.4 V, desorbing at +0.4 V	10	10.4	0.8	107
	20	10.9	1.4	92
	40	10.3	1.3	97

independent of its concentration and of the potential change.

In general the bed of graphite granules was not removed from the Vycor tube between experiments but when fresh graphite was used it was found to adsorb a quantity of lysozyme quite independently of potential. Once absorbed, this material appeared to be permanently incorporated on the bed and was some 4 times the weight of the electrosorption. Following this natural adsorption there appeared to be no limit to the number of potential-dependent adsorption–desorption cycles. When the bed was initially saturated with a solution of a second protein, trypsin, the ratio of the natural to electrosorption fell to 1:1.

The lysozyme loading measurement was repeated using the nephelometer as detector and the longer Vycor tube cell. With 100 ppm lysozyme a loading of 4.3 mg was obtained, in good agreement with the spectrophotometric figures. This demonstrated that the protein was not degraded in the adsorption–desorption cycle i.e. the spectrophotometer was not following the concentration of an amino acid from the protein.

3.3. *Sorption of bacteria*

The same experimental arrangement was then used with a suspension of *Serratia marcescens* in 0.01 M Na_2SO_4. Again the familiar adsorption–desorption cycle was detected, only at the opposite polarity to the lysozyme, i.e. the bacteria were adsorbed anodically and desorbed cathodically. Fig. 5 shows the trace obtained at ±0.8 V. The desorption peak is dependent on the preceding adsorption time but, unlike the lysozyme, it is smaller than the adsorption. This would not be surprising if there were any change in the dimensions or state of aggregation of the bacteria.

Table 3. Weight of lysozyme adsorbed in the larger cell

Solution concentration (ppm)	*Flow rate (ml min^{-1})*	*Loading (mg)*
40	10.9	4.3
80	8.4	3.9
120	11.4	4.5

3.3.1. Bacteriacidal effect. Fig. 6 shows the counts obtained when 0.01 M Na_2SO_4 supporting electrolyte was used through the twin bedded cell of Fig. 1 when infected solution was passed through the two beds and the potential reversed every minute during the collection of samples 2 to 6. In each case there is a significant reduction in the bacterial population in the centre of the figure. The volume of the cell and outlet pipe give the lag between the fall and rise in counts and the period of application of the alternating potential. The observed reduction in the live bacterial population with the application of an alternating potential indicates that some if not all of the bacteria which undergo the adsorption–desorption cycle are killed.

Fig. 7 shows the counts obtained for two successive runs where a solution of 5 g l^{-1} peptone in 0.01 M Na_2SO_4 was substituted for the 0.01 M Na_2SO_4. In the first there is a distinct drop between samples 3 and 4 as was observed in Fig. 6, though this effect is much reduced. In the second run this drop is scarcely perceptible. These results indicate that the adsorption sites on the graphite are preferentially filled with the

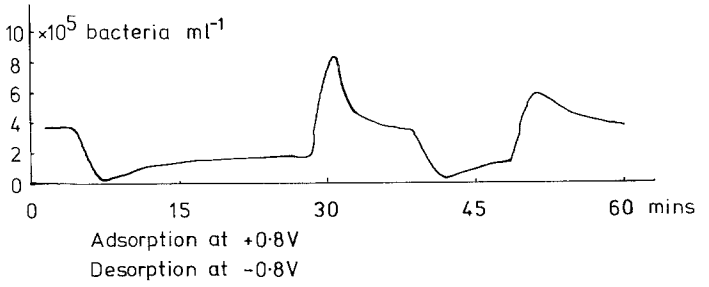

Fig. 5. Adsorption and desorption of *Serratia marcescens* from a suspension in 0.01 M Na_2SO_4.

peptone which is not desorbed and consequently no bacteria can be adsorbed so that they therefore pass through the cell unaffected. The possibility that SO_2 is picked up during initial sterilization and discharged during the application of a potential is ruled out as similar results might then be expected with and without the peptone.

3.4. *Bed material and pretreatment*

Having established that a wide range of materials could be adsorbed onto and desorbed from a graphite bed by control of the applied potential, a variety of bed materials and pretreatments were tested to investigate means of improving the loading for a given weight of bed material to give a more compact device. Solutions of 40 ppm lysozyme were used in conjunction with the flat bed cell as this was the most convenient to reload.

Fig. 8 shows the dependence on particle size of the loading of lysozyme. Sieves of 45, 90, 150, 250, 500 and 710 μm were employed to separate ground EY110 graphite. The loading was determined on each fraction and the graphite

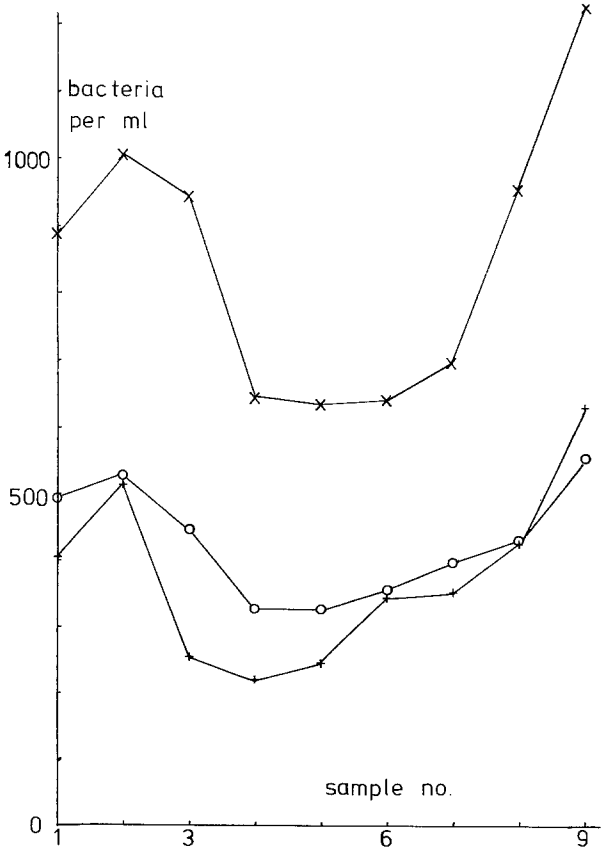

Fig. 6. Bacteria per ml in the samples collected from the twin bed cell across which 4 V were applied, the polarity being reversed every minute during the collection of samples 2–6 inclusive. The bacteria were suspended in 0.01 M Na_2SO_4. Results from three separate runs.

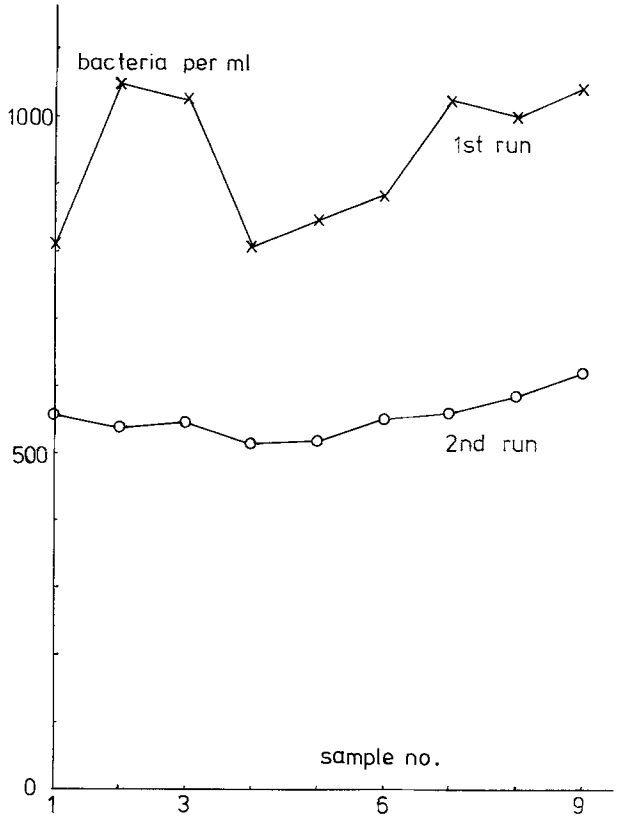

Fig. 7. Bacteria per ml in the samples collected from the twin bed cell. The bacteria were suspended in 5 g l^{-1} peptone in 0.01 M Na_2SO_4, but the other experimental arrangements were identical with those of Fig. 6. Results from two separate runs.

removed from the cell, dried and weighed. The linear dependence on the reciprocal of the particle diameter is that which would be expected from the increase in the surface areas of the graphite. However, the use of very fine particles presents practical difficulties, firstly with containment and secondly with the pressure drop required for a given flow rate.

Samples of Le Carbone-Lorraine graphite flakes, Morganite carbon wool (7501C) and graphite wool (7501G) were examined. The fibres have a diameter of 8 μm and therefore give a much larger surface area per unit weight than was attainable with a sieved powder. The loading measured in $\mu g\, g^{-1}$ is given for these samples and a variety of pretreatments in Table 4.

Activated carbon was tested but it was found impossible to make the bed negative despite the passage of large currents for long periods. This was assumed to be due to the substantial uptake of oxygen during the process of activation, which it was first necessary to reduce. The same problem was encountered with the graphite wool heated in oxygen at 800° C for 2 h; negative potentials were effectively unattainable.

Several points emerge from the table. Firstly, the fibres do not give the improvement anticipated from their increased surface area. Secondly, treatment with sulphuric acid, chlorosulphonic acid, nitric acid, thionyl chloride and bromine all increase the loading over the untreated material or the material treated with hydrogen peroxide. This improved effect was lost by prolonged reduction at -1.0 V. All these reagents should form intercalation compounds with the graphite which should be destroyed with the formation of a residue compound when the graphite is returned to water. Though this residue compound has the same X-ray structure as the original graphite it retains many of the intercalated ions [10], i.e. bisulphate in the case of the sulphuric acid treatment. The intercalation compound is formed by attack along the edges of the graphite layer planes.

Oxygen entirely destroys the effect, though the

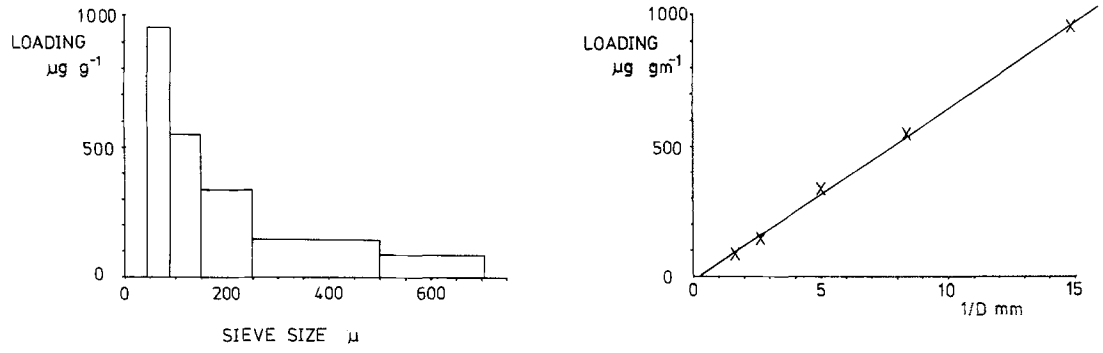

Fig. 8. Dependence of loading on particle size, plotted first as an histogram and secondly as the reciprocal of the average sieve size (D) vs loading.

oxygen taken up at 350° C may be reduced until the loading is as good as that attainable with the sulphuric acid treatment alone. Hennig [11] found that surface oxides on graphite crystals formed by exposure to oxygen were not present on the cleavage surfaces but were present only on the edge atoms, which also indicates that it is at these same edge sites that the adsorption–desorption phenomenon takes place.

Table 4. Effect of pretreatment on loading

Sample and treatment	*Loading μg g⁻¹*
EY 110 graphite powder, 45–90 μm, H_2SO_4 treatment	956
Le Carbone graphite flakes, H_2SO_4 treatment	262
Morganite graphite wool 7501G	
As received	36
H_2SO_4 treatment	350
Reduce above at −1.0 V for 12 h	36
Heat in O_2 at 350° C for 12 h, H_2SO_4 treatment	172
Reduce above at −1.0 V for 4 h	225
Reduce above at −1.0 V for 8 h	479
Reduce above at −1.0 V for 12 h	394
Heat in O_2 at 800° C for 2 h	–
Heat in CO_2 at 1000° C for 2 h	182
As above with H_2SO_4 treatment	495
Reflux in 30% H_2O_2 for 1 h	30
Reflux in 70% HNO_3 for 8 h	272
Reflux in $SOCl_2$ for 1 h	143
Reflux in Br_2 for 1 h	132
Morganite Carbon Wool 7501C	
H_2SO_4 treatment	705
Heat in CO_2 at 1000° C for 2 h, H_2SO_4 treatment	1180

Heating in carbon dioxide improved the loading with both graphite and carbon wools; however, heating ground graphite in carbon dioxide for 1 h roughly halved its capacity. Harker *et al.* [12] found that annealing graphite powder for 1 h in vacuum reduced its reactivity with oxygen to about half its initial value. They concluded that mechanical damage centres were formed on powdering which were a type of dislocation and accounted for the reactivity lost on annealing. In the case of the fibres no mechanical damage centres can be present as they are produced by carbonization of extruded synthetic fibres. The carbon dioxide treatment may increase the loading by pitting the fibre and increasing the active surface area.

Carbon fibre gives distinctly better results than graphite fibre though both are lower than might be expected from the fibre diameter and the extrapolation of the figures for powdered graphite. These fibres are produced for mechanical strength and the graphite lamellae are oriented along the length of the fibre thus minimizing the exposure of the edges of the planes. To avoid this structure (which is initiated in the extrusion of the artificial fibre precursor) in commercial carbon and graphite fibres, a natural fibre, cotton wool, was carbonized, firstly in a stream of nitrogen to 450° C and then to 900° C in streams of argon or carbon dioxide. These products were very friable and appeared to contain many inorganic impurities, but a loading figure was estimated from the desorption band of 2929 and 3590 $\mu g\, g^{-1}$ for the samples carbonized in argon and carbon dioxide respectively.

4. Discussion

The results in Table 4 demonstrate that the adsorption–desorption sites are at the edges of the graphite layer planes. This is suggested by the improvement obtained in loading with the residue compounds left after subjecting the graphite to an intercalating agent and confirmed by the influence of oxygen. Once oxygen is taken up at the edge sites the phenomenon can no longer occur. The importance of these sites explains the superior performance of the powdered graphite to the fibres and flakes.

The edge sites on graphite are known to be terminated in a variety of functional groups, the nature of which depends on the pretreatment [13]. However, the sorption processes reported here do not appear to depend on a particular functional group as greater differences might have been expected between the loading figures obtained on graphite fibres after treatment with such a wide variety of intercalating agents. It is at these sites that the phenomenon occurs, however, and bearing in mind the observed sorption of OH^- ions it would appear that any functional group which is capable of supplying or retaining an OH^- ion will be a useful contributor to the sites available for the electrosorption process. Such an hypothesis would go some way to explaining the lack of dependence of the loading on solution concentration.

5. Conclusion

The potential-dependent sorption which occurs on a packed bed electrode of graphite is quite different from that observed on metal surfaces [14] and permits a wide range of materials from molecules to bacteria to be added, retained, and discharged at will. The active sites for this process are the edges of the graphite layer planes.

The loading appears independent of concentration and OH^- ion sorption also occurs, which suggests the retention mechanism is similar to that of an ion exchange bed. However, the balance between adsorption and desorption is controlled by modification of the pK of the surface functional groups with the applied potential rather than a change of the pH of the eluting solvent.

The phenomenon could obviously find application to a very wide range of separation problems, for example analysis, the separation of reaction mixtures and possibly even filtration. However, it is very unselective so that despite the ability to kill *Serratia marcescens* this bacteriacidal effect is lost in the presence of other adsorbable materials and therefore the device is unlikely to find application as a sterilizer.

Acknowledgement

We are grateful for a research fellowship from Carlson-Ford (now APV-Carlson) and also for their permission to publish this work.

References

[1] E. K. Rideal, 'An Introduction to Surface Chemistry', Cambridge University Press (1926) Chap. 7.
[2] G. Horanyi, *J. Electroanal. Chem.* **51** (1974) 163.
[3] J. S. Newman and C. W. Tobias, *J. Electrochem. Soc.* **109** (1962) 1183.
[4] G. J. Hills, *Chem. Br.* **12** (1976) 291.
[5] J. B. Goodall, MPhil thesis, University of Southampton (1976).
[6] J. H. Strohl and K. L. Dunlap, *Anal. Chem.* **44** (1972) 2166.
[7] R. C. Alkire and R. S. Eisinger, *J. Electrochem. Soc.* **130** (1983) 85.
[8] J. H. Strohl and K. Sexton, *Sep. Sci.* **9** (1974) 557.
[9] D. Gilroy and J. E. O. Mayne, *J. Appl. Chem.* **12** (1962) 382.
[10] K. E. Carr, *Carbon* **8** (1970) 155.
[11] G. R. Hennig, *Fifth Carbon Conference* **1** (1961) 143.
[12] H. Harker, J. B. Horsley and Robson, *Carbon* **9** (1971) 1.
[13] J. B. Donnet, *Carbon* **6** (1968) 161.
[14] S. Trasatti, *J. Electroanal. Chem.* **53** (1974) 335.